

A Preliminary Study on Dynamic Airspace Configuration Using Flexible Vertical Boundaries in Double-Layer Airspace

Harutaka Suizu[1,2], Hiroko Hirabayashi[1], & Noboru Takeichi[2]

[1]Air Traffic Management Department, Electronic Navigation Research Institute

[2]Graduate School of Systems Design, Tokyo Metropolitan University

Abstract

The radar control airspace in the Fukuoka Flight Information Region (FIR) was reorganized into a two-layer structure separated by FL335. This study focuses on the Kobe Area Control Center (ACC) and investigates boundary altitude optimization by varying the vertical separation altitude. The Kobe ACC was divided into three operational areas, and the optimal boundary altitudes were identified as FL315, FL295, and FL335 for Areas A, B, and C, respectively. To interpret these differences, traffic-flow analysis using trajectory clustering, ADOI-based labeling, and workload distribution metrics (R_{upper} and Cf_{upper}) was conducted. The results suggest that optimal boundary altitude cannot be fully explained by traffic volume alone and is also influenced by traffic-flow structure, with workload redistribution closely associated with the characteristics of major traffic flows. Area-wise analysis identifies distinct workload-formation patterns: Area A exhibits competing flows, Area B shows vertical role separation, and Area C is dominated by large-scale overflight traffic. These findings indicate that boundary altitude should be interpreted as an emergent property of traffic-flow structure, reflecting the organization of vertical traffic-flow roles between upper and lower sectors.

Keywords: Dynamic Airspace Configuration; ATC Workload; Traffic Flow Structure Analysis

1. Introduction

In conventional air traffic control operations, services are provided based on fixed air routes within airspace units configured with predetermined geometries. Airspace capacity has traditionally been improved by subdividing sectors and limiting the number of aircraft handled within each sector. However, the coexistence of cruising aircraft and climbing/descending aircraft within the same sector has posed challenges in further improving operational efficiency and increasing the number of aircraft that can be handled.

To address this issue, domestic en-route airspace in the Fukuoka Flight Information Region (FIR), where Japan provides air traffic control services, was reorganized between fiscal years 2018 and 2024. As a result, a vertically separated two-layer structure was introduced with a boundary altitude of FL335, dividing the airspace into high-altitude sectors primarily handling cruising aircraft and low-altitude sectors mainly handling climbing and descending traffic.

However, the boundary altitude is currently operated as a fixed value across the entire airspace, and may not necessarily be optimal under varying traffic conditions and operational environments. Additionally, interviews with air traffic controllers have reported cases in which unexpected sector transfers occurred due to prediction errors in climb profiles, leading to increased coordination tasks and controller workload.

In recent years, the concept of Dynamic Airspace Configuration (DAC), which enables flexible modification of airspace structures in response to traffic demand, has been proposed. DAC is an operational concept in which sector configurations, including their shapes and structures, are dynamically adjusted based on predicted traffic flow. The introduction of DAC has been incorporated into the Global Air Navigation Plan of the International Civil Aviation Organization (ICAO) as a means

to improve air traffic control efficiency and increase airspace capacity [1]. In Japan, it is also being considered as one of the long-term initiatives in the Collaborative Actions for Renovation of Air Traffic Systems (CARATS 2040), the long-term vision for air traffic system development [2]. Within this context, dynamic adjustment of boundary altitude is regarded as a key element for realizing DAC.

However, the effectiveness of boundary altitude adjustment inherently depends on the structural characteristics of traffic flow. Existing studies have primarily focused on aircraft-count-based mathematical optimization or workload-based evaluation using indices such as the Modified-Messerschmidt, Bölkow und Blohm (MMBB) method. In contrast, the structural characteristics of traffic flow—particularly traffic-flow structure—and their influence on boundary altitude and airspace configuration have not been sufficiently investigated. In other words, a structural understanding of why specific boundary altitude becomes effective remains unresolved.

In this study, the Kobe Area Control Center (ACC) in the Fukuoka FIR is investigated, focusing on the relationship between traffic-flow structure and boundary altitude. Optimization simulations were conducted for multiple scenarios in which the boundary altitude was varied from FL215 to FL415 in 2,000-ft increments. Based on these simulations, appropriate boundary altitudes were examined from the perspective of air traffic control workload. Furthermore, the target airspace was divided into several operational areas based on controller qualification areas and traffic-flow characteristics. For each area, suitable boundary altitudes were derived, and the applicability of dynamic boundary altitude adjustment was evaluated.

The objective of this study is to propose a boundary altitude determination framework that considers both the structural characteristics of traffic flow and operational constraints, and to provide fundamental insights for airspace operation design toward the practical implementation of DAC in Japan.

The main contributions of this study are summarized as follows:

(1) It is shown that optimal boundary altitude cannot be fully explained by traffic volume alone and is strongly associated with traffic-flow structure.

(2) The limitations of workload-only interpretations are discussed, and a traffic-flow structure-based interpretation framework for airspace design is proposed.

(3) The feasibility of dynamic boundary altitude adjustment under operational constraints at the ACC and controller qualification level is investigated, providing operational insights for practical implementation.

This paper is organized as follows. Section 2 reviews the current air traffic management framework and related studies. Section 3 describes the data used in this study. Section 4 presents the proposed methodology for boundary altitude optimization and flow-level analysis. Section 5 presents the results and discusses the effectiveness of the proposed approach. Finally, Section 6 concludes the paper.

2. Background and literature review

2.1 Airspace Structure and Operations

En route air traffic control operations refer to the management of aircraft flying at higher altitudes, excluding airspace in the vicinity of airports, where air traffic controllers monitor aircraft positions using radar surveillance and ensure safe separation through control instructions, thereby maintaining an orderly traffic flow between aircraft operating between airports and those traversing Japanese airspace [3]. As of March 2025, the radar-controlled airspace in the Fukuoka FIR has been reorganized into a vertically separated two-layer structure, divided into high- and low-altitude sectors with a boundary altitude at FL335. The high-altitude sectors primarily handle cruising aircraft, while the low-altitude sectors mainly handle climbing and descending aircraft as well as short-haul traffic.

Figure 1 illustrates the vertically separated structure along representative flight trajectories for the Tokyo–Fukuoka route, which has the highest traffic volume in Japan [4]. Aircraft depart from the Tokyo metropolitan area, climb through the TMA and the low-altitude sector, and subsequently transition to the high-altitude sector.

DAC is a concept that enables flexible modification of airspace configurations in response to traffic demand, aiming to optimize airspace capacity by adjusting boundary altitude and sector structures. While sector merging and splitting based on traffic demand are already implemented in Japan, these operations largely rely on air traffic controllers' experience, and systematic design methodologies remain limited.

In addition, Japanese airspace is characterized by high-density traffic flows within a confined region, making it important to account for regional traffic-flow characteristics in airspace design. Therefore, rather than relying on a fixed boundary altitude, more flexible airspace operations that adapt to traffic-flow structure are required. Designing boundary altitude configurations that reflect traffic-flow characteristics remains a key challenge.

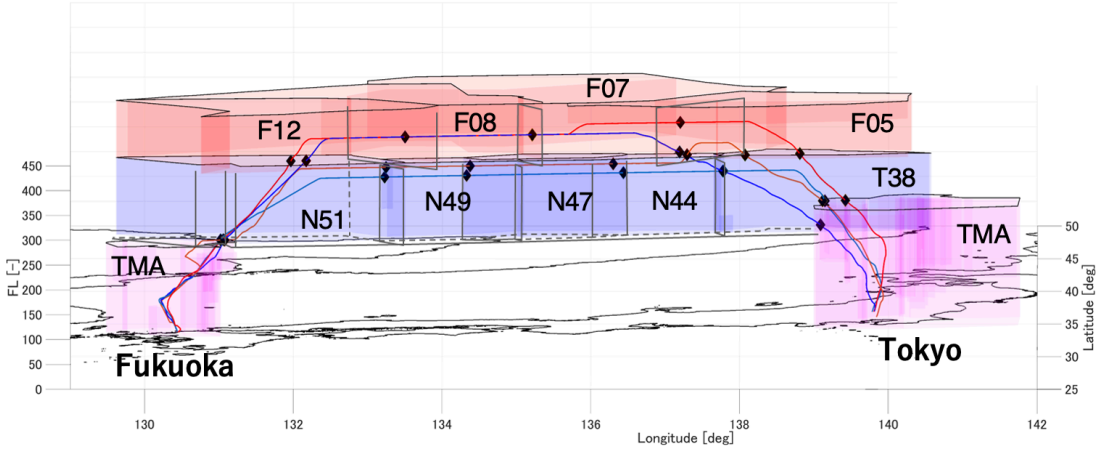


Figure 1 – Vertically separated airspace structure and representative flight trajectories for the Tokyo–Fukuoka route.
Magenta indicates the TMA, blue the low-altitude sectors, and red the high-altitude sectors.

2.2 Dynamic Airspace Configuration in Airspace Management

DAC is an internationally recognized framework for airspace management in which sector configurations are flexibly adjusted in response to traffic demand to improve operational efficiency. It is positioned as a key component of next-generation air traffic management in the ICAO Global Air Navigation Plan [1].

In Japan, DAC has also been identified as a key initiative in the CARATS 2040 roadmap for air traffic system development. Within this framework, adjustment of boundary altitude and restructuring of sector configurations are recognized as essential elements for implementing DAC [2]. These two types of airspace configuration changes—boundary altitude adjustment and horizontal sector restructuring— are conceptually illustrated in Fig. 2.

Among these, boundary altitude adjustment reallocates control responsibility between upper and lower sectors according to traffic distribution, thereby improving airspace capacity and balancing controller workload. However, the boundary altitude is currently operated as a fixed value despite variations in traffic conditions and traffic-flow characteristics among airspace regions. Therefore, establishing a systematic framework for determining appropriate boundary altitudes that accounts for both traffic-flow characteristics and operational constraints remains a key challenge for realizing DAC.

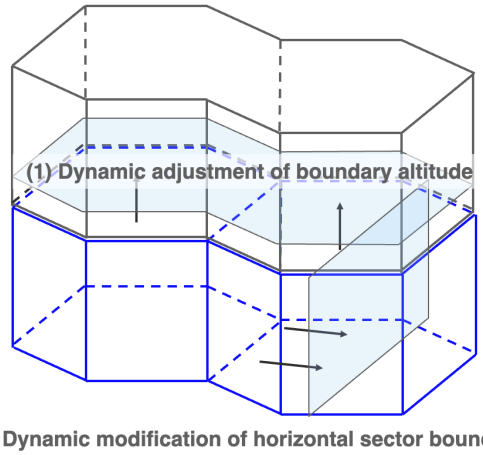


Figure 2 – Conceptual illustration of airspace configuration changes in DAC:
(1) Dynamic adjustment of boundary altitude
(2) Dynamic modification of sector boundaries in the horizontal plane.

2.3 Model of Workload Index for Air traffic Control (ATC)

Air traffic management (ATM) aims to ensure safe and efficient use of airspace by regulating traffic flow when traffic demand is expected to exceed airspace capacity [3]. In practice, traffic flow control measures, such as departure regulation (e.g., Calculated Take-Off Time, CTOT) [5], are applied based on predicted traffic conditions to maintain safe separation and orderly traffic flow.

In Japanese airspace, such traffic flow control is based on air traffic control workload, evaluated using the MMBB method. In this method, the workload generated by each aircraft is estimated as the product of a unit control workload derived statistically from historical traffic data and the dwell time of the aircraft within a sector.

Traffic flow control is applied proactively based on predicted traffic conditions. The ATC workload, denoted as WL [s], is calculated every 10 minutes from forecast traffic over a 30-minute look-ahead period (1800 seconds). For each aircraft f flying within a given sector during the evaluation period, the workload is computed as the product of the unit control workload $Ctld$ [s/min] and the predicted dwell time $t_{pred,\ f}$ [min] derived from forecast traffic. The total workload is then obtained by summing over all IFR aircraft $\mathbb{A}$ within the sector, as expressed in Eq. (1):

$$WL = \sum_{\mathbb{A} \ni f} Ctld \cdot t_{pred,\ f} \tag{1}$$

The airspace capacity is defined as the evaluation period length (1800 seconds), and traffic flow control measures are applied when the predicted workload exceeds this capacity. This value is used as a nominal threshold under normal conditions.

The unit control workload $Ctld$ is defined as the time required for a controller to handle a single aircraft flying within a sector for one minute [6]. Since instruction frequencies vary depending on sector and traffic characteristics, $Ctld$ is assigned as a sector-specific parameter. Furthermore, instruction frequency depends on the flight phase. Flight operations are classified into four categories: Arrival (A), Departure (D), Inner (I), and Overflight (O), and are further distinguished between jet and propeller aircraft. Consequently, eight distinct unit control workload values are defined for each sector.

2.4 Literature Review: Workload-based Airspace Optimization

The concept of DAC was initially proposed to enable flexible airspace reconfiguration in response to traffic demand, aiming to mitigate demand–capacity imbalance and improve operational efficiency [7]. Since then, research on airspace design has primarily focused on air traffic control workload evaluation and mathematical optimization.

Most existing studies optimize airspace configuration using sector-level ATC workload as a performance metric. Various approaches, including metaheuristic optimization and mathematical programming, have been proposed to adjust sector boundaries and improve airspace capacity and workload balance [8, 9].

In the context of Japanese airspace, previous studies have evaluated the effects of boundary altitude changes on airspace capacity, as well as examined workload estimation based on the MMBB method and actual control command data [10, 11].

However, these studies have limited consideration of the structural characteristics of traffic flow. In particular, the relationship between traffic-flow structure and airspace configuration has not been systematically investigated. As a result, the role of traffic-flow structure in determining appropriate boundary altitude remains insufficiently understood.

2.5 Literature Review: Flow-based Analysis

Trajectory-based clustering has been widely used to analyze air traffic-flow structures. Various approaches have been proposed, including clustering of full trajectories, extraction of representative flow units based on entry and exit points, and flow identification using density-based methods such as Density-Based Spatial Clustering of Applications with Noise (DBSCAN) or probabilistic models such as Gaussian Mixture Models (GMM) [12–15].

However, these approaches have inherent limitations for ACC-scale airspace analysis. Even traffic flows that share common entry and exit points may exhibit multiple operational patterns due to differences in altitude-transition behavior and routing variations. Conversely, clustering based on full-trajectory similarity may lead to excessive segmentation, as the results strongly depend on spatial distance and density, potentially dividing operationally similar flows.

Therefore, existing clustering approaches face limitations in representing both operationally meaningful traffic flow units and their internal structure simultaneously. As a result, it remains difficult to systematically interpret the influence of traffic-flow structure on boundary altitude determination.

3. Data used

3.1 Actual Trajectory Data

In this study, trajectory data provided by the Civil Aviation Bureau of Japan, covering the period from April 2024 to March 2025, were used. The dataset includes time-series aircraft position information (timestamp, latitude, longitude, and pressure altitude) for flights operating within the Fukuoka FIR and partially in adjacent FIRs. In addition, flight operation information, such as origin airport, destination airport, flight identification, and aircraft type, is included.

The data source is the Trajectorized En-route Traffic Data Processing System (TEPS), which integrates multi-sensor data, including radar information, with a temporal resolution of approximately 2 seconds. To reduce noise, trajectory smoothing was applied based on the method described in [16], followed by linear interpolation to ensure uniform temporal spacing.

To ensure data confidentiality, flight-specific identifiers such as Flight Object ID (FOID) and flight numbers were anonymized before analysis.

3.2 ADP (Adaptation Data)

In this study, Adaptation Data (ADP), which includes information required for air traffic control operations—such as sector definitions, FIX points, and airway configurations—were used. Specifically, sector definition data and unit control workload parameters obtained from the Flight Object Administration Center System (FACE) were applied.

The dataset corresponds to the AIRAC (Aeronautical Information Regulation and Control) cycle issued on March 20, 2025, representing the operational configuration after the completion of vertical airspace separation within the Fukuoka FIR.

3.3 Analysis Period and Target Scope

The analysis period was defined for two seasons: summer (June 1, 2024–September 30, 2024; 122 days) and winter (December 1, 2024–March 31, 2025; 121 days). This study focuses on the Kobe Area Control Center (ACC) within the Fukuoka FIR, as shown in Fig. 3, which consists of 11 sectors. The Tokyo metropolitan area, a major origin and destination of traffic, is highlighted by a red circle to indicate its influence on traffic patterns

Based on controller qualifications and traffic-flow characteristics, the Kobe ACC was grouped into three operational areas, hereafter referred to as Areas A, B, and C, each comprising three to five sectors. Among the five sectors in Area A, sectors N47 and N49 were excluded from the analysis because their boundary altitudes are operationally fixed and differ from FL335.

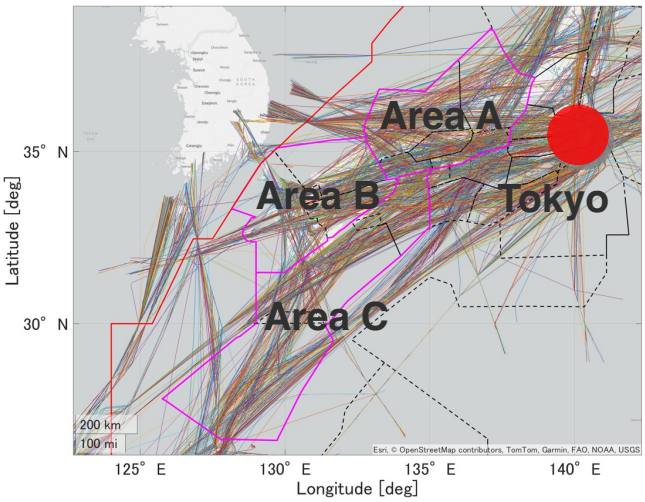


Figure 3 – Overview of Kobe ACC (magenta)
(Trajectory: 2024/08/01)

4. Methodology

Figure 4 shows the overall methodology of this study. First, boundary altitude optimization was performed using an MMBB-based workload evaluation for each operational area (Areas A, B, and C). The optimal boundary altitude was explored by balancing workload distribution between high- and low-altitude sectors. Next, representative traffic-flow structures were extracted using trajectory clustering based on spatial trajectory features. The extracted flows were then labeled using statistics based on flight operational categories, where each flight was classified into one of four categories: Arrival (A), Departure (D), Overflight (O), and Inner (I). Based on the distribution of these categories. Based on the distribution of these categories (referred to as ADOI), the workload contributions of the upper and lower sectors were evaluated for each subflow. Finally, the relationship between traffic-flow structure and workload distribution was analyzed to interpret how flow characteristics shape the formation of the optimal boundary altitude.

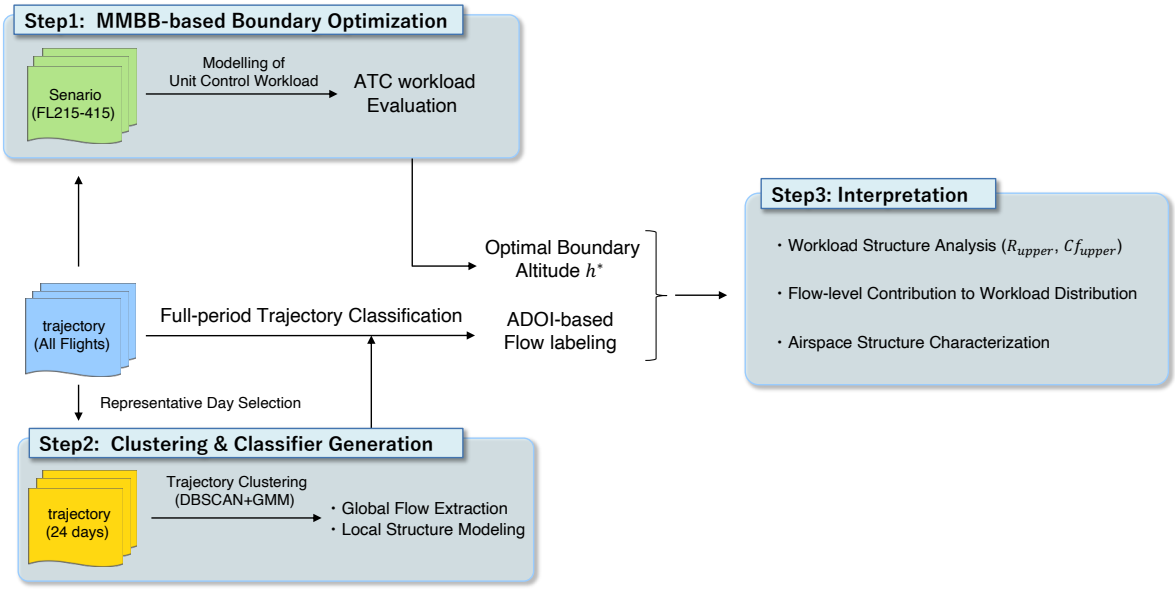


Figure 4 – Overall framework for flow-level interpretation of boundary altitude optimization

4.1 Overview of Boundary Altitude Optimization Simulations

This section describes the boundary altitude optimization process shown in Fig. 4. Boundary altitude configurations were systematically evaluated to identify the optimal setting for each operational area (Areas A, B, and C). The optimal boundary altitude between the high-altitude and low-altitude sectors was determined based on the following two criteria using workload data for both sectors obtained from simulations with varying boundary altitudes:

(i) Minimization of the total air traffic control workload of the high- and low-altitude sectors.

(ii) Minimization of the workload difference between them, ensuring balanced workload distribution.

The boundary altitude satisfying these criteria is defined as the optimal boundary altitude h^*.

In this study, boundary altitude was treated as an analysis parameter, while assuming that the climb and descent positions of aircraft are independent of the boundary altitude. This assumption is considered reasonable, as climb and descent are typically conducted based on aircraft requests under normal operations.

The evaluation domain consists of the low-altitude sector L_1 assigned to the Kobe ACC and the airspace immediately above it within the high-altitude sectors H_i (Fig. 5), representing the region where workload is redistributed between upper and lower sectors as the boundary altitude changes.

The analysis was performed for three operational areas (Areas A, B, and C). Simulations were conducted by varying the boundary altitude from FL215 to FL415 in 2000-ft increments. For each boundary altitude, sector dwell time was calculated and used to estimate workload for the low-altitude sector and the aggregated high-altitude sectors.

The workload of each sector was calculated based on the unit control workload $Ctld$, derived from historical traffic statistics, as defined in Section 2.3. To account for boundary altitude changes, the unit control workload was adjusted according to the relative position of the boundary altitude, assuming proportionality to both the vertical extent of the controlled altitude band and the sector area. When defining unit control workload at the revised boundary altitude FL', the following assumptions were introduced:

(i) Control workload is assumed to be proportional to both the vertical width of the controlled altitude band and the sector area.

(ii) Control operations for areas no longer within the jurisdiction due to boundary altitude

changes are transferred to the corresponding low- or high-altitude sector (Fig. 6).

(iii) Airspace below FL200 is primarily controlled by the Terminal Management Area (TMA), and the number of flights operating above FL430 is negligible. Therefore, the primary altitude bands controlled by the low- and high-altitude sectors are FL200-FL430.

The baseline unit control workload is defined under the current operational condition at FL335. Accordingly, the adjusted unit control workload for other boundary configurations was derived as a function of the relative position of the boundary altitude, as described by Eqs. (2)-(5). The low-altitude sector under evaluation is denoted by L_1, the aggregated high-altitude sectors by H_{all}, and the high-altitude sector directly above L_1 by H_i. The area common to both sectors is denoted by A_{com}, and the sector areas are denoted by A_{L_i} and A_{H_i}, respectively.

$(FL' \geq FL335)$

$$Ctld_{H_i}{}' = Ctld_{H_i} \cdot \frac{FL430-FL'}{FL430-FL335} \quad (2)$$

$$Ctld_{L_1}{}' = Ctld_{L_1} + \sum_{H_i \in H_{all}} Ctld_{H_i} \cdot \frac{FL'-FL335}{FL430-FL335} \cdot \frac{A_{com}}{A_{H_i}} \quad (3)$$

$(FL' < FL335)$

$$Ctld_{H_i}{}' = Ctld_{H_i} + Ctld_{L_1} \cdot \frac{FL335-FL'}{FL335-FL200} \cdot \frac{A_{com}}{A_{L_1}} \quad (4)$$

$$Ctld_{L_1}{}' = Ctld_{L_1} \cdot \frac{FL'-FL335}{FL335-FL200} \quad (5)$$

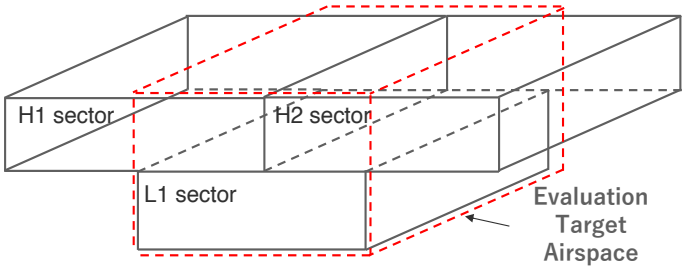


Figure 5 – Evaluation target airspace of High-altitude sector and Low-altitude sector. (H_i: High-altitude sector, L1: Low-altitude sector)

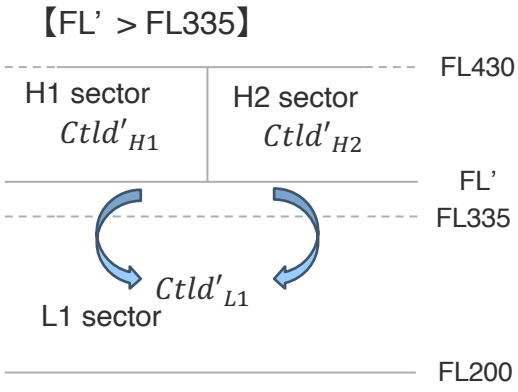


Figure 6-1 – Switching over the workload from Higher to Lower Sector

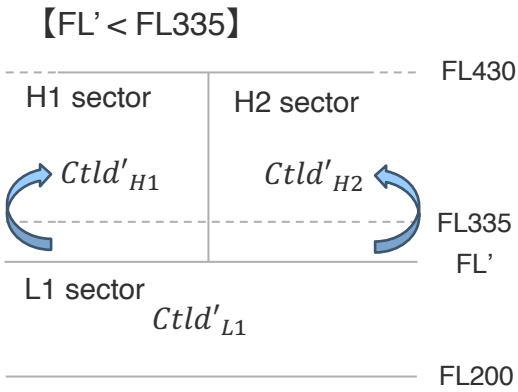


Figure 6-2 – Switching over the workload from Lower to Higher Sector

4.2 Flow Clustering

This section describes the flow extraction and clustering process shown in Fig. 4. While the optimal boundary altitude can be determined using an MMBB-based ATC workload evaluation, the underlying factors that shape this optimum are not explicitly revealed. In particular, the relationship between traffic-flow structure and controller workload cannot be directly interpreted from aggregated workload metrics. Therefore, in this study, trajectory clustering is applied to represent traffic as a set of representative flow units, enabling interpretation of how traffic-flow structure is associated with the formation of the optimal boundary altitude at the flow level.

Lindner et al. [15] proposed a method for extracting traffic flow funnels by applying additional clustering within coarse clusters to reveal their internal structure. Following this concept, this study adopts a two-stage clustering approach, considering that multiple operational patterns may exist within each coarse traffic cluster. A distinguishing feature of this study is the use of a GMM to represent internal traffic-flow structures probabilistically.

Specifically, global traffic flow patterns are first extracted using DBSCAN to identify coarse clusters. Then, GMM is applied within each cluster to model detailed subflow structures. This hierarchical approach enables the capture of both large-scale traffic organization and fine-grained operational variations.

4.2.1. DBSCAN: Global Flow Extraction

In this study, DBSCAN was applied to trajectory data to extract the global structure of traffic flows. DBSCAN was selected because it does not require prior specification of the number of clusters and can effectively identify noise and low-density regions in heterogeneous trajectory data.

For clustering, each trajectory was represented by its entry and exit positions within the target airspace together with its overall heading direction.

Entry and exit positions were transformed into planar coordinates $(x, \ y)$, and the heading angle was incorporated using $(\cos\theta \quad \sin\theta)$ to preserve directional continuity. Altitude information was not directly used in the clustering process, and classification was performed based on horizontal trajectory shape and direction. Accordingly, each trajectory was represented by the feature vector shown in Eq. (6).

$$(x_{in} \quad y_{in} \quad x_{out} \quad y_{out} \quad \cos\theta \quad \sin\theta) \tag{6}$$

After standardizing the features, DBSCAN was applied using the Euclidean distance. The minimum number of samples required to form a cluster $(minPts)$ was set to 20, and the neighborhood radius ε was determined for each area based on clustering stability and noise characteristics.

The clusters extracted by DBSCAN are defined as coarse clusters (cluster1), and trajectories classified as noise were excluded. This enables the extraction of representative large-scale traffic-flow structures within each operational area.

4.2.2. GMM: Local Structure Modeling

To capture variability within each coarse cluster, Gaussian Mixture Models (GMM) were applied to represent subflow structures probabilistically.

Prior to clustering, trajectories were transformed into fixed-length feature vectors representing trajectory shape and direction. Each trajectory was resampled along its normalized path length and represented as a sequence of spatial points along with heading direction information, resulting in a 42-dimensional feature vector. Dimensionality reduction was performed using principal component analysis (PCA) to mitigate redundancy and correlation among features. This data-driven approach reduces reliance on predefined flow classes and enables subflows to be extracted from the underlying structure of the traffic data.

Based on the GMM results, each trajectory was assigned to the subflow with the highest posterior probability. Samples with low assignment confidence were excluded.

The clustering results from DBSCAN and GMM were subsequently used as a flow classification model to assign traffic flows to representative traffic-flow structures for analysis.

4.3 Flow labeling

In this study, a flow classifier was constructed based on the clustering results obtained from representative-day data in Section 4.2 and applied to trajectories over the entire analysis period. The feature representation is identical to that used in the clustering process, consisting of resampled spatial coordinates and heading direction. Each trajectory is first assigned to a coarse cluster (cluster1) based on entry and exit positions, followed by projection into the corresponding PCA space. Within this space, fine-level classification (cluster2) is performed by assigning trajectories to the nearest Gaussian component. Distance-based thresholds are applied at both stages to exclude trajectories that deviate significantly from existing traffic-flow structures. Through this procedure, each trajectory is assigned a hierarchical flow label (cluster1–cluster2), which is used for subsequent flow-level analysis.

To provide operational interpretation of the extracted traffic-flow structures, flow-level labeling is performed using flight operational categories. Each trajectory is classified into one of four categories: Arrival (A), Departure (D), Overflight (O), and Internal (I), based on its origin–destination airport information.

Specifically, a list of ADOI-related airports is defined for each operational area by aggregating the airports associated with the corresponding sectors. A trajectory is classified as Departure (D) if only the origin airport is included in the ADOI list, Arrival (A) if only the destination airport is included, Overflight (O) if neither airport is included, and Internal (I) if both airports are included.

It should be noted that ADOI information is assigned after clustering for interpretability and is not used as a clustering feature. This allows the extracted traffic-flow structures to be analyzed independently of flight operational categories while providing an operational interpretation of each subflow. The resulting ADOI compositions are used for subsequent workload analysis.

4.4 Workload Structure Metrics

To evaluate the contribution of each subflow to the upper/lower workload structure, two metrics were defined. First, the upper-sector occupancy tendency of subflow f was defined:

$$R_{upper,f} = \frac{WL_{upper,f}}{WL_{upper,f}+WL_{lower,f}} \tag{7}$$

where $WL_{upper,f}$ and $WL_{lower,f}$ denote the workload generated by subflow f in the upper and lower sectors, respectively. Here, $WL_{upper,f}$ and $WL_{lower,f}$ are derived by decomposing the sector-level workload WL defined in Section 2.3 into subflow-level contributions. $R_{upper,\ f}$ represents the degree to which a subflow is handled by the upper sector. Larger values indicate that the flow is predominantly processed in the upper sector.

Next, the relative contribution of subflow f to the total upper-sector workload was defined as:

$$Cf_{upper,f} = \frac{WL_{upper,f}}{\sum_f WL_{upper,f}} \tag{8}$$

where $\sum_f W_{upper,f}$ represents the total workload of the upper sector aggregated over all subflows. $Cf_{upper,\ f}$ represents the relative contribution of each subflow to the total upper-sector workload. These metrics are used to characterize the contribution of each subflow to the workload distribution between the upper and lower sectors.

5. Results and Discussions

5.1 Optimal Boundary Altitude

In this study, boundary altitude configurations ranging from FL215 to FL415 were evaluated for each area in 2,000-ft increments. For each configuration, time-series data of ATC workload were obtained under both summer and winter conditions. Table 1 summarizes the current and identified optimal boundary altitudes for each operational area, while Figures 7–9 present the ATC workload ratio relative to airspace capacity for Areas A, B, and C. In these figures, the blue bars represent the total workload across upper and lower sectors, whereas the orange bars represent the workload difference between them.

Under current operations, the boundary altitude is fixed at FL335. However, the identified optimal boundary altitude differs across areas. In Area A, FL315 was identified because it provided the most balanced workload distribution between the upper and lower sectors, while in Area B, both the total workload and workload difference were minimized at FL295. In contrast, Area C showed an optimal boundary altitude of FL335, consistent with the current operational setting. Furthermore, the identified optimal boundary altitude was consistent across both summer and winter conditions in all areas, suggesting that seasonal traffic variation has a limited influence on the results.

These findings highlight that the optimal boundary altitude varies systematically across areas despite similar evaluation criteria, suggesting that it cannot be fully explained by aggregated workload metrics alone. In particular, the structural characteristics of traffic flow are considered to shape the distribution of workload between upper and lower sectors, potentially contributing to the formation of distinct optimal boundary altitudes. This relationship is further examined in the following sections.

Table 1 – Current and identified optimal boundary altitudes for each operational area

Area	Current	Identified optimal
A	FL335	FL315
B	FL335	FL295
C	FL335	FL335

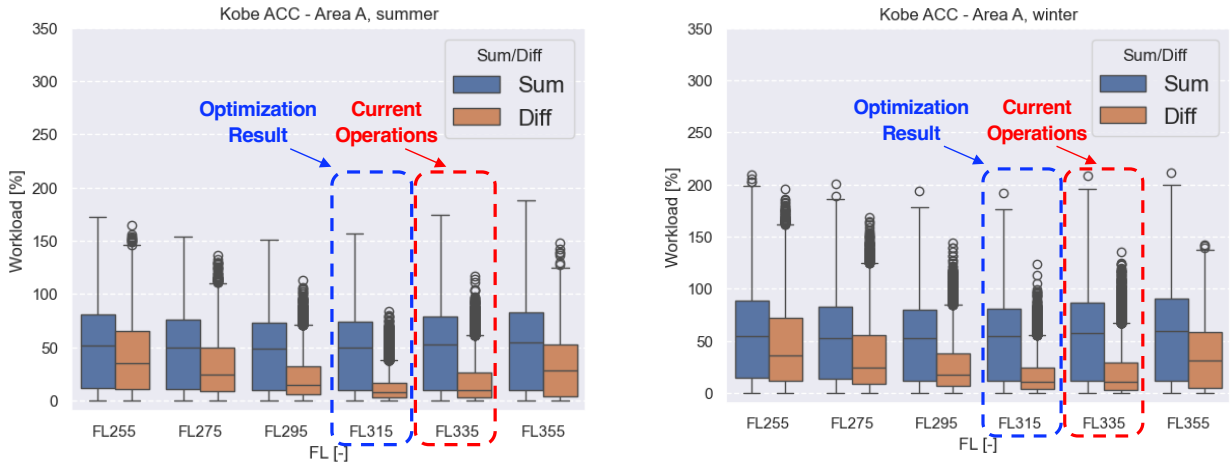


Figure 7 – ATC workload as a ratio to airspace capacity (Area A)
(left figure: summer, right figure: winter)

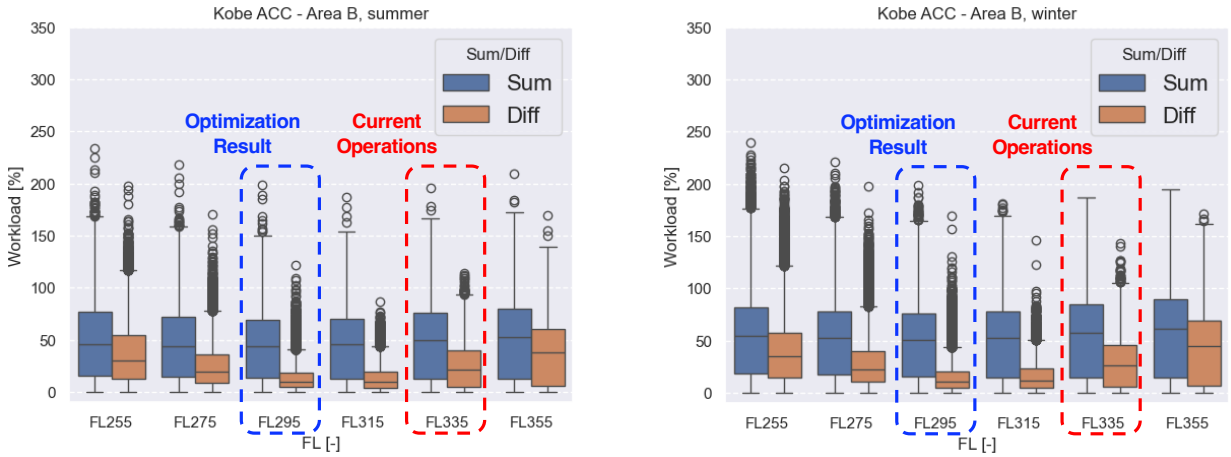


Figure 8 – ATC workload as a ratio to airspace capacity (Area B)
(left figure: summer, right figure: winter)

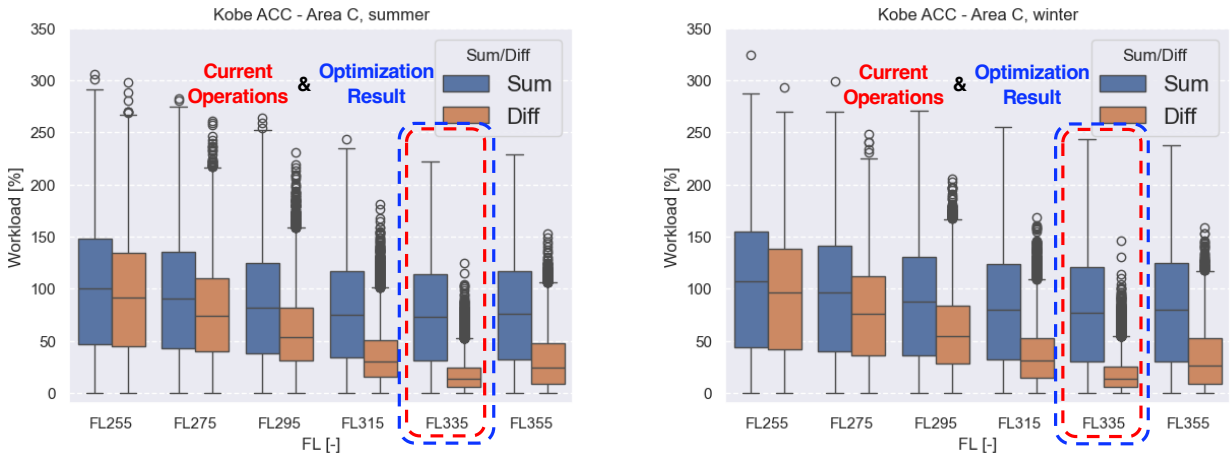


Figure 9 – ATC workload as a ratio to airspace capacity (Area C)
(left figure: summer, right figure: winter)

5.2 Traffic-flow Structure Analysis

This section analyzes the traffic-flow structures extracted through clustering. For each area, coarse clusters and subflows were identified using DBSCAN and GMM, and their operational interpretation was further examined based on ADOI classification.

Figure 10 shows representative examples of the extracted subflows obtained by applying the classifier to the entire trajectory dataset. The extracted subflows exhibit spatially consistent structures across the analysis period, indicating that the identified traffic-flow patterns are reproducible beyond the representative-day dataset. Furthermore, analysis of the ADOI composition indicates that each subflow is typically dominated by a specific operational category, such as Overflight (O), Arrival (A), or Departure (D), suggesting that the extracted subflows correspond to distinct operationally meaningful traffic-flow structures.

Although multiple subflows can exist within a single coarse cluster, they exhibit distinct spatial and operational characteristics, indicating that heterogeneous traffic patterns are embedded within similar large-scale traffic-flow structures.

A comparison across areas highlights clear differences in traffic-flow structure. Area A contains a mixture of competing flow patterns, Area B is dominated by relatively uniform overflight traffic, and Area C consists of a combination of large-scale overflight and internal arrival/departure flows.

These findings indicate that traffic-flow structures differ significantly across areas, suggesting that such structural differences shape the distribution of workload between upper and lower sectors. While ADOI classification provides an operational interpretation of traffic based on origin–destination information, the clustering-based approach reveals spatial and structural characteristics that cannot be distinguished using ADOI categories alone. These traffic-flow structures provide the basis for the workload analysis presented in the following section.

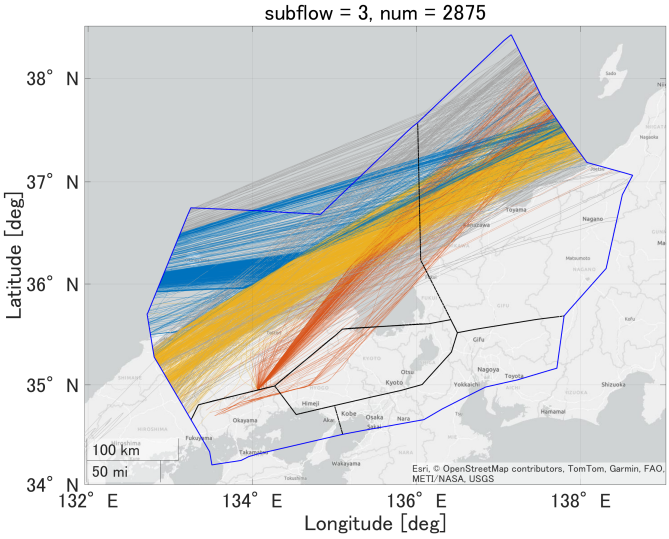


Figure 10 – Representative DBSCAN coarse cluster (Cluster1 ID = 3) in Area A and its corresponding GMM-derived subflows
(Subflows are shown in blue, orange, and yellow; outliers are shown in gray)

5.3 Flow Contribution to Workload

This section analyzes how each traffic flow contributes to ATC workload, based on the subflow structures and ADOI classification identified in Section 5.2. In particular, the upper-sector occupancy ratio $R_{upper,f}$ and the workload contribution ratio $Cf_{upper,f}$ at the optimal boundary altitude h^* are examined to evaluate flow-level workload characteristics. Because changes in boundary altitude directly redistribute traffic and workload between upper and lower sectors, these metrics provide a useful means of examining how traffic-flow structure shapes workload distribution and contributes to

the formation of different optimal boundary altitudes.

Figure 11 presents the relationship between $R_{upper,f}$ and $Cf_{upper,f}$ for each subflow in each area. Each point corresponds to a subflow; the color indicates the Overflight ratio (ratio_O), and the marker size represents the total workload ($WL_{upper,f} + WL_{lower,f}$). Table 2 summarizes the top five subflows that contribute most to the upper-sector workload in each area.

Subflows located in the upper-right region of Fig. 11 exhibit both high upper-sector occupancy and high workload contribution, indicating a strong influence on upper-sector workload. In contrast, subflows in the lower-left region contribute relatively little to the upper-sector workload and are primarily associated with lower-sector operations. Intermediate positions indicate flows that distribute workload across both sectors and are therefore particularly relevant to workload allocation around the boundary altitude. The color represents the proportion of Overflight traffic, with higher values indicating overflight-dominant traffic.

Area A exhibits a "competitive" structure, in which multiple subflows contribute to workload formation across a broad range of intermediate $R_{upper,f}$ values. In this configuration, no clear dominance of either the upper- or lower-sector workload contribution is observed, and multiple flows compete in shaping workload allocation around the boundary altitude. As shown in Fig. 11(a), subflows are distributed over a wide range of $R_{upper,f}$ values rather than being concentrated in a specific region. This tendency is also reflected in Table 2-1, where subflows with strong upper-sector contributions and those contributing to the lower sector coexist within a similar $R_{upper,f}$ range.

Area B exhibits a "separated" structure, in which upper- and lower-sector workload are generated by distinct groups of traffic flows. As shown in Fig. 11(b), Overflight-dominant flows are concentrated at high $R_{upper,f}$ and primarily contribute to upper-sector workload, whereas Arrival- and Departure-dominant flows are concentrated at low $R_{upper,f}$ values and contribute mainly to lower-sector workload. This clear separation of functional roles is also supported by Table 2-2, where major flows are strongly biased toward either the upper or lower sector, indicating a stable division of workload responsibilities.

Area C exhibits a "dominant" structure, in which a limited number of traffic flows account for a disproportionately large share of the upper-sector workload. As shown in Fig. 11(c), a small number of Overflight-dominant flows with high ratio_O values generate a large fraction of the upper-sector workload. Table 2-3 shows that individual subflows can contribute more than 10% of the total upper-sector workload, indicating the presence of dominant high-altitude traffic corridors. In contrast, lower-sector workload is distributed among multiple Arrival- and Internal-dominant flows.

Overall, upper-sector workload is primarily generated by Overflight-dominant traffic, whereas lower-sector workload is mainly associated with Arrival- and Departure-related traffic. However, the manner in which these flows interact differs substantially across areas. The competitive, separated, and dominant structures identified in Areas A, B, and C therefore represent distinct patterns of workload formation arising from differences in traffic-flow structure.

These results demonstrate that ATC workload formation differs substantially across areas because it is strongly related to the interactions and role distributions of multiple traffic flows rather than any individual traffic flow. These differences in workload structure help explain why the identified optimal boundary altitude varies across areas. Although the optimal boundary altitude is obtained through workload-based evaluation, this analysis suggests that the underlying structure of that workload is shaped by traffic-flow characteristics. Therefore, boundary altitude should be interpreted as an emergent property of traffic-flow structure rather than a parameter determined solely by aggregate workload metrics. In this study, a flow-structure-based interpretation framework is proposed to explain how traffic-flow characteristics shape workload distribution and contribute to the formation of the optimal boundary altitude.

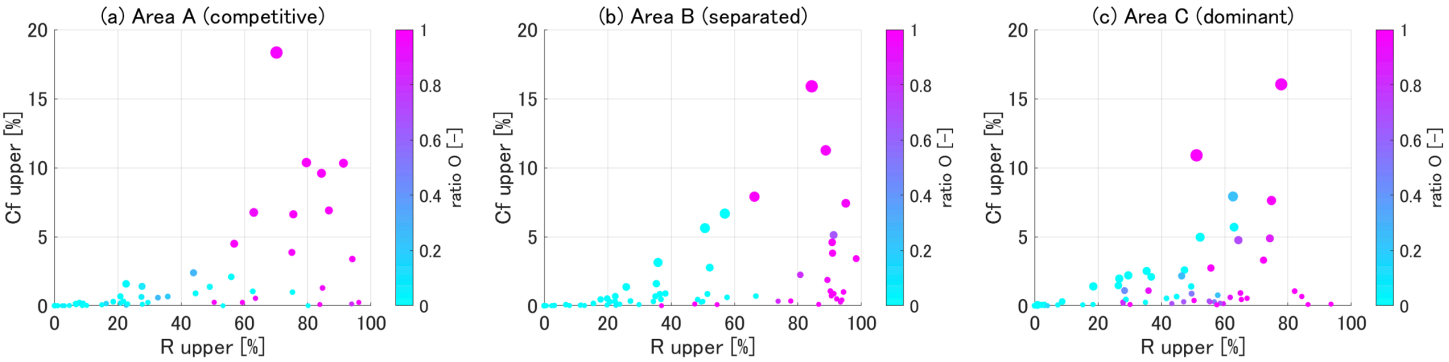


Figure 11 – Relationship between upper-sector occupancy ($R_{upper,f}$) and workload contribution ($Cf_{upper,f}$) for each subflow at the optimal boundary altitude. (Each point represents a sub-flow; color denotes ratio O; marker size indicates total workload)

Table 2-1 – Top contributing subflows to upper-sector workload in Area A (sorted by $Cf_{upper,f}$)

subflow	Cf_{upper}	R_{upper}	ratio_O
A-1-1	18.3	70.1	0.975
A-3-3	10.4	79.6	0.996
A-3-1	10.3	91.3	1.000
A-5-4	9.6	84.3	1.000
A-2-2	6.9	86.7	0.999

Table 2-2 – Top contributing subflows to upper-sector workload in Area B (sorted by $Cf_{upper,f}$)

subflow	Cf_{upper}	R_{upper}	ratio_O
B-2-2	15.9	84.3	1.000
B-2-1	11.3	88.8	0.980
B-4-1	7.9	66.3	0.993
B-2-3	7.4	95.1	0.960
B-1-1	6.7	56.9	0.000

Table 2-3 – Top contributing subflows to upper-sector workload in Area C (sorted by $Cf_{upper,f}$)

subflow	Cf_{upper}	R_{upper}	ratio_O
C-3-1	16.0	77.8	0.965
C-2-1	10.9	51.1	1.000
C-3-2	7.9	62.2	0.233
C-3-3	7.6	74.8	0.996
C-9-1	5.7	63.0	0.025

6. Conclusion and Future Work

This study evaluated alternative boundary altitude configurations for Kobe ACC Areas A, B, and C using MMBB-based workload evaluation and identified area-specific optimal boundary altitudes. In addition, a traffic-flow-based interpretation of optimal boundary altitude formation was developed. To interpret the relationship between traffic-flow structure and upper- and lower-sector workload distributions, traffic flows were extracted using trajectory clustering based on DBSCAN and GMM. In addition, ADOI-based flow labeling and workload structure metrics were introduced to evaluate how individual subflows contribute to workload formation under different boundary altitude configurations.

The results indicate that the optimal boundary altitude cannot be fully explained by traffic volume alone and is also influenced by the structure of traffic flows and their associated workload distribution. While workload-based optimization identified different optimal boundary altitudes for Areas A, B, and C, the proposed flow-level analysis suggests that these differences are associated with distinct traffic-flow structures and their contributions to upper- and lower-sector workloads.

Area-wise analysis showed distinct traffic-flow structures associated with different optimal boundary altitudes. Area A exhibits a competitive structure, in which multiple competing overflight and transition flows contribute to workload formation around the boundary altitude. This results in strong boundary sensitivity, particularly in the FL295–315 range, where multiple flows interact across altitude layers. Area B exhibits a separated structure, characterized by a clear division of workload roles between overflight and arrival/departure traffic. The resulting separation between a stable upper-sector overflight corridor and lower-sector transition flows contributes to a relatively low optimal boundary altitude. In contrast, Area C exhibits a dominant structure, in which a limited number of overflight traffic flows account for a large proportion of the upper-sector workload. This dominance of large-scale, high-altitude overflight traffic contributes to the selection of a higher optimal boundary altitude around FL335.

Therefore, optimal boundary altitude should be interpreted not merely as a static means of minimizing workload, but as an emergent property of the organization of vertical traffic-flow roles between upper and lower sectors. The flow-structure-based interpretation framework proposed in this study explains why different airspace regions require different boundary altitude configurations and provides insights for dynamic airspace configuration in vertically separated airspace.

Future work will focus on extending the proposed framework to broader airspace configurations and evaluating its applicability across varying traffic-demand scenarios and operational constraints. In addition, the workload redistribution model adopted in this study is based on several simplifying assumptions, and further validation of these assumptions remains an important subject for future research.

Acknowledgement

The authors would like to acknowledge the Japan Civil Aviation Bureau for providing the data used in this study. The authors are also grateful to the staff of the Tokyo Air Traffic Control Center, Kobe Air Traffic Control Center, Fukuoka Air Traffic Control Center, and the Air Traffic Management Center for their valuable insights into air traffic control operations and ATM systems obtained through interviews and investigations.

Contact Author Email Address

Contact Author: Harutaka Suizu

Email: suizu-h@mpat.go.jp

Copyright Statement

The authors confirm that they, and/or their company or organization, hold copyright on all of the original material included in this paper. The authors also confirm that they have obtained permission, from the copyright holder of any third-party material included in this paper, to publish it as part of their paper. The authors confirm that they give permission, or have obtained permission from the copyright holder of this paper, for the publication and distribution of this paper as part of the ICAS proceedings or as individual off-prints from the proceedings.

References

[1] ICAO. *Global Air Navigation Plan (GANP)*, Doc 9750, 6th edition, International Civil Aviation Organization, Montreal, Canada, 2022.

[2] Japan Civil Aviation Bureau. Collaborative Actions for Renovation of Air Traffic Systems 2040 (CARATS 2040) Roadmap. Available at https://www.mlit.go.jp/koku/carats/ (accessed May 23, 2026).

[3] Japan Civil Aviation Bureau. Overview of air navigation services (2025). Available at https://www.mlit.go.jp/koku/content/001743241.pdf (accessed May 23, 2026). (in Japanese)

[4] Suizu H, Hirabayashi H, Brown M, Murata A, Imuta T and Takeichi N. Initial analysis of sector patterns after airspace reorganization in Fukuoka FIR. Proc *63rd The Japan Society for Aeronautical and Space Sciences Aircraft Symposium*, Naha, Japan, Oct. 17, 2025. (in Japanese)

[5] Japan Civil Aviation Bureau. *Air traffic control procedure regulations No. 5 (effective March 20, 2025)*, 2025. (in Japanese)

[6] Hirabayashi H, Brown M, Murata A, Suizu H and Imuta T. Identifying issues in air traffic flow management for air traffic in en-route sector separated by altitude. Proc *Asia-Pacific International Symposium on Aerospace Technology (APISAT 2025)*, Seoul, South Korea, 2025.

[7] Kopardekar P, Bilimoria K and Sridhar B. Initial concepts for dynamic airspace configuration. Proc *7th AIAA Aviation Technology, Integration and Operations Conference (ATIO)*, Belfast, Northern Ireland, Sep. 2007.

[8] Sergeeva M, Delahaye D, Mancel C and Vidosavljevic A. Dynamic airspace configuration by genetic algorithm. *Journal of Air Transport Management*, Vol. 63, pp 300-314, 2017.

[9] Saruwatari Y, Izunaga Y, Ukai T and Kageyama K. Two optimization approaches for airspace configuration. Proc *19th Electronic Navigation Research Institute Symposium*, Tokyo, Japan, 2019. (in Japanese)

[10] Hirabayashi H, Brown M, Imuta T and Murata A. Traffic characteristics and impact on capacity management in altitude-separated sector airspace. Proc *62nd Aircraft Symposium*, Fukui, Japan, 2024. (in Japanese)

[11] Murata A, Hirabayashi H and Imuta T. Study on workload monitoring for fatigue management in air traffic control. Proc *62nd The Japan Society for Aeronautical and Space Sciences Aircraft Symposium*, Fukui, Japan 2024. (in Japanese)

[12] Murça M C R, Hansman R J, Li L and Ren P. Flight trajectory data analytics for characterization of air traffic flows: a comparative analysis of terminal area operations between New York, Hong Kong and Sao Paulo. *Transportation Research Part C*, Vol. 97, pp 324-347, 2018.

[13] Basora L, Morio J and Mailhot C. A trajectory clustering framework to analyse air traffic flows. Proc *7th SESAR Innovation Days*, 2017.

[14] Kajikawa R and Takeichi N. Feasibility study on landing capacity enhancement at congested airports via arrival trajectory analysis. Proc *57th The Japan Society for Aeronautical and Space Sciences Annual Meeting*, 2026. (in Japanese)

[15] Lindner M, Zeh T, Braßel H and Fricke H. Aircraft performance-optimized departure flights using traffic flow funnels. Proc *14th USA/Europe Air Traffic Management R&D Seminar (ATM2021)*, 2021.

[16] Bach R E and Paielli R A. A user guide for smoothing air traffic radar data. *NASA/TM-216520*, 2024.